Journal of Power Sources 249 (2014) 385–391

Contents lists available at ScienceDirect

Journal of Power Sources

journal homepage: www.elsevier.com/locate/jpowsour

Improved performance of dye-sensitized solar cells with novel conjugated organic dye using aluminum oxide-coated nanoporous titanium oxide films

Hyo Jeong Jo [a], Jung Eun Nam [a], Dae-Hwan Kim [b], Jin-Kyu Kang [a,*]

[a] Advanced Convergence Research Center, DGIST, Hyeonpung-Myeong, Daegu 711-873, South Korea
[b] Division of Energy, DGIST, Hyeonpung-Myeong, Daegu 711-873, South Korea

HIGHLIGHTS

- We reported our findings on solution-process-deposited Al_2O_3 barriers in DSSCs.
- We focused on the effect that adsorption properties of dye can have on the interfacial charge transfer reactions.
- These results were supported by the Raman spectroscopy, IMPS and IMVS.

ARTICLE INFO

Article history:
Received 30 July 2013
Received in revised form
27 September 2013
Accepted 14 October 2013
Available online 1 November 2013

Keywords:
Aluminum oxide barriers
Titanium oxide/dye/electrolyte interface
Tunneling
Dye adsorption
Dye-sensitized solar cells

ABSTRACT

This work introduces the TiO_2/dye/electrolyte interface in the recombination and offers an interface treatment method using solution process for dye-sensitized solar cells (DSSCs). Solution-processed ultra-thin metal oxides introduce to treat the surface of mesoporous TiO_2 to reduce the defect density and improve the electronic quality. Among the metal oxides, an Al_2O_3 barrier is incorporated into DSSCs as a carrier-recombination blocking layer. In all instances, the short-circuit current density increase and the dark current is suppressed after Al_2O_3 deposition. The impact of the Al_2O_3 barriers is also studied in devices employing different dyes. To compare the behavior of metal-free organic dyes and Ru dyes when Al_2O_3 barrier layers are involved, the charge transfer between the dye and TiO_2 electrodes, associated with interfacial electron injection, is investigated by Raman spectroscopy. The metal-free organic dye had a high molar extinction coefficient and better adsorption properties compare to Ru dye, which resulted in higher charge-collection efficiency. To verify the strategy, the DSSCs photovoltaic performances containing these dyes are compared using their current–voltage curves. Electrochemical impedance spectroscopy (EIS), Intensity Modulated Photocurrent Spectroscopy (IMPS), and Intensity Modulated photoVoltage Spectroscopy (IMVS) were used to further investigate the kinetics process of the TiO_2 film electrodes.

1. Introduction

Since the historic paper on dye-sensitized solar cells (DSSCs) was published in 1991 by Grätzel et al., DSSCs have been widely investigated because of their special advantages such as low fabrication costs and fairly high solar-energy-conversion efficiencies relative to conventional p–n junction solar cells [1,2]. In DSSCs, dye molecules are chemisorbed on the surface of a TiO_2 porous layer, and visible light is absorbed by the sensitizer dye to generate excited electrons. Electron injection from the excited state of the dye into the conduction band of TiO_2 is followed by subsequent regeneration of the dye by an I^-/I_3^- redox couple [3–5]. Efficient operation of a DSSC device relies upon the minimization of possible recombination pathways occurring at the TiO_2–dye–electrolyte interface, allowing efficient charge transport through the TiO_2 film and electrolyte and subsequent charge collection at the device contacts. There are two possible recombination losses to consider: the injected electrons may recombine either with oxidized dye molecules or with the oxidized redox couple; the latter reaction is thought to be particularly critical to device function (Scheme 1) [6].

In order to reduce the recombinations, many research groups have proposed device architectures that include the use of insulating polymers. The use of very thin-layered, high band-gap,

* Corresponding author. Tel.: +82 53 785 3700; fax: +82 53 785 3739.
E-mail address: apollon@dgist.ac.kr (J.-K. Kang).

0378-7753/$ – see front matter © 2013 Elsevier B.V. All rights reserved.
http://dx.doi.org/10.1016/j.jpowsour.2013.10.051

semiconductor metal oxides like ZnO, MgO, and Al_2O_3 between the TiO_2 and the dye interface has also been attempted [6–11]. The application of a metal-oxide barrier layer should improve the collection efficiency of electrons successfully injected into TiO_2 by reducing the number of charge carriers lost via recombination. Aluminum oxide is especially attractive owing to its wide bandgap [8], high iso-electric point (IEP, which can enhance dye adsorption) [8,12], and ability to raise the TiO_2 conduction band edge (which can improve the open-circuit voltage, V_{oc}) [13]. On the other hand, the high conduction band of Al_2O_3 will inhibit electron injection from an excited dye state into TiO_2. Therefore, if the Al_2O_3 barrier layer is too thick, the device current will drop as relaxation of the dye excited state competes with electron injection via tunneling.

In this paper, we reported our findings on solution-process-deposited Al_2O_3 barriers in DSSCs. In order to reduce the defect density and improve the electronic quality, solution-processed ultra-thin metal oxides have been introduced to treat the surface of mesoporous TiO_2 [14]. In addition, we focused on the effect that adsorption properties of sensitizer can have on the interfacial charge transfer reactions and ultimately on the device efficiency. We illustrated, as an example, adsorption properties by sensitizer affect not only to increase the electron injection efficiency but also to slow recombination on the Al_2O_3-coated TiO_2 electrode compared to TiO_2 electrode. By comparing the behavior of the Ru dye and a metal-free organic dye, we demonstrated the importance of dye chemistry on current collection (Fig. 1).

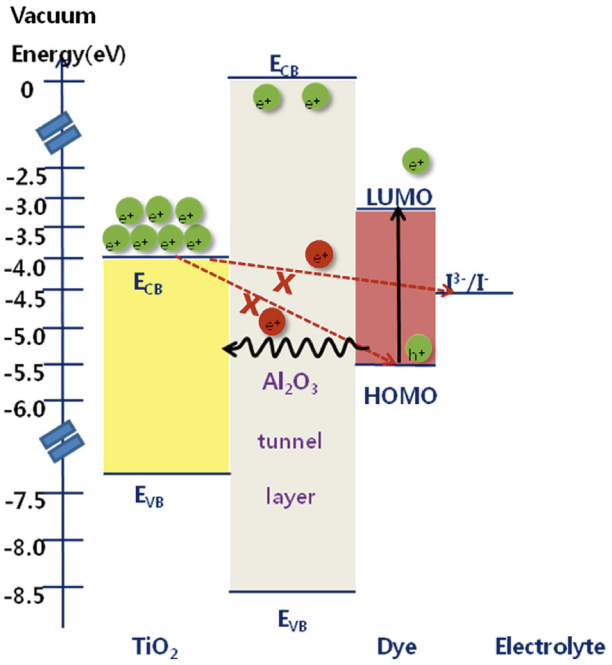

Scheme 1. Illustration of interfacial charge-transfer processes in DSSCs.

2. Experimental details

2.1. Fabrication of DSSC using Al_2O_3

In order to prepare a working electrode, fluorine-doped thin oxide (FTO) for a conductive transparent electrode was purchased from Pilkington ($\sim 8\ \Omega\ sq^{-1}$) and cleaned using the general cleaning process for electronic applications: ultrasonic treatment in detergent, deionized water, acetone, and 2-propanol in that order for 15 min for each at room temperature. The transparent and porous titanium oxide film was formed on the cleaned FTO substrate using 20-nm particle-size TiO_2 paste (Solaronix, T/SP) with the doctor-blade coating method. The coated TiO_2 film was sintered at 500 °C in air for 60 min. An air-stable solution of aluminum 2-propoxide (15 mM in isopropanol) under aerobic conditions was used to conformally coat the TiO_2. The film was dipped in the coating solution for 15 min at 25 °C. After this, the film was dried to water vapor for 1 min at 100 °C. For dye adsorption, the Al_2O_3-coated TiO_2 electrodes were immersed in a dye solution (0.3 mM of dye in ethanol) at room temperature for 24 h. The dye-adsorbed TiO_2 electrode and Pt counter electrode were assembled using 60-μm-thick Surlyn (Dupont, 1702) as a bonding agent. A liquid electrolyte was introduced through a pre-punctured hole on the counter electrode.

2.2. Synthesis of PREDCN2 dye

We designed and synthesized organic dyes containing a phenothiazine derivative as an electron donor and a cyanoacrylic acid moiety as an electron acceptor and anchoring group, connected with electron-rich ethylene-di-oxythiophene (EDOT) as a π-conjugated group in a chromophore with moderate yields. The synthetic procedures were followed using known methods [15–17]. The product obtained was a dark red powder. Yield: (0.48 g, 81.3%), ^{1}H NMR (400 MHz, DMSO-d_6): δ 8.01 (s, 2H), 7.50–7.48 (d, J = 8.4 Hz, 2H), 7.38–7.37 (d, J = 2.0 Hz, 2H), 7.35–7.33 (d, J = 8.4 Hz, 2H), 7.20–7.17 (m, 2H), 6.12–6.01 (d, J = 8.8 Hz, 2H), 2.71–2.65 (m, 2H), 1.64–1.53 (m, 4H), 1.33–1.30 (m, 4H), 0.88 (m, 3H). MALDI-TOF MS: Calcd. for $C_{44}H_{35}N_3O_8S_3$ m/z: 829.16; found m/z: 830.85 $[M+H]^+$; anal. calcd. for C: 63.67; N: 5.06; S: 11.59; H: 4.25; found, C: 63.86; N: 5.58; S: 11.29; H: 4.68%.

2.3. Characterization of physical, electrochemical, and electrical properties

The morphologies of Al_2O_3 coated TiO_2 electrode were measured using transmission electron microscopy (TEM, Hitachi HF-3300).

Structural analysis was conducted using ^{1}H NMR spectra recorded via a Bruker Advance NMR 400 Hz spectrometer for DMSO-d_6. Matrix Assisted Laser Desorption Ionization-Time Of Flight mass spectra were obtained using a Voyager DE-STR spectrometer. UV–Vis spectra were recorded using a CARY5000 UV/Vis/NIR spectrophotometer. The redox properties were examined using cyclic voltammetry (model: Iviumstate). The electrolyte solution was 0.1 M tetrabutyl ammonium hexafluorophosphate (TBAPF6) in freshly dried dimethylformamide (DMF). Ag/AgCl and platinum wire (0.5 mm in diameter) electrodes were used as reference and counter electrodes, respectively.

Raman spectra were obtained using an Almega XR Raman spectrometer (Thermo scientific) with 532 nm solid-state laser.

The photocurrent-density–voltage characteristic of the DSSCs was measured using a Keithley 2400 source meter and a solar simulator equipped with a 1 kW xenon arc lamp (ORIEL, Newport). A standard silicon solar cell (PV Measurement Inc.) was used for calibration with the power of the AM 1.5 simulated light (100 mW cm^{-2}).

To perform electrochemical impedance spectroscopy (EIS), the DSSCs were measured under dark condition by a potentiostat (IVIUM, Iviumstat); the frequency range was from 0.1 Hz to 100 kHz. The data obtained from this measurement was fitted by simulation software (Scribner Associates, Z-View), which proposed an equivalent circuit to model the data. Intensity Modulated Photocurrent Spectroscopy (IMPS) and Intensity Modulated

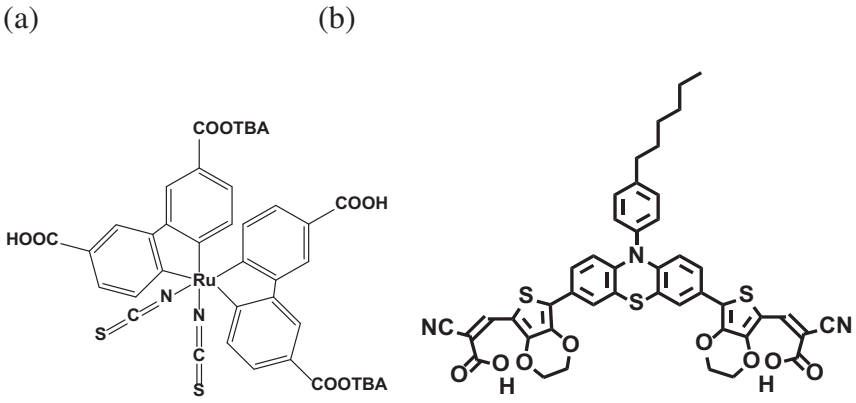

Fig. 1. Molecular structures of (a) N719 (TBA: tetra-*n*-butylammonium cation) and (b) PREDCN2.

photoVoltage Spectroscopy (IMVS) were measured by a potentiostat (IVIUM, Iviumstat).

3. Results and discussion

3.1. Characterization of optical, electro-chemical, and electrical properties

HRTEM analysis shows the formation of the Al_2O_3 layer over TiO_2 particles. The magnified HRTEM images of TiO_2–Al_2O_3 after the solution process are given in Fig. 2. In order to analyze the distribution of Al_2O_3 on the porous TiO_2 layer surface, EPMA measurement was carried out. These images show ultra-thin film formation around TiO_2, with an Al_2O_3 layer thickness of 0.4 nm [18]. EPMA color mapping shows Al was distributed uniformly on the TiO_2 layer surface. This indicated that Al_2O_3 was filled-up pores on the TiO_2 surface. The uniform distribution of Al_2O_3 on the TiO_2 layer increase an electron injection efficiency by tunneling.

In order to investigate the effect of the Al_2O_3 layer on the rectification of the interface, we measured the EIS spectra under dark conditions, and the results are shown in Fig. 3.

The EIS spectra were analyzed through a well-known equivalent circuit [19–21]. The EIS plots of the bare and Al_2O_3-coated samples had two semicircles. The one in the high-frequency region was assigned to the charge-transfer process at the counter electrode. The charge-transfer resistance at the counter electrode was almost the same for both bare and Al_2O_3-coated samples with different dyes. The second arc denoted the resistance at the TiO_2–dye–electrolyte interface, the resistance for the transport of electrons to the conduction glass electrode for the bare sample, and also the change in the interface resistance for the sample with Al_2O_3 between TiO_2 and the dye. The increased resistance for the samples after Al_2O_3 coating indicated acceleration of the electron transport process in the photo anode by preventing charge recombination at the TiO_2–dye–electrolyte interface. In particular, PREDCN2 devices with the Al_2O_3 layer do not suffer from a high recombination rate compared with bare TiO_2 devices. One possibility for the low recombination rate could be the manner in which the PREDCN2 dye was attached to the Al_2O_3-coated TiO_2 surface, in which the mode of anchoring of dye onto the photoelectrode affected the electron injection efficiency and hindered access of the electrolyte.

In order to study the interaction between dye molecules and the TiO_2 surface, which was associated with interfacial electron injection, we analyzed the Raman spectra of the one-layered TiO_2 electrode, shown in Fig. 4.

It is worth noting that strong Raman peaks corresponding to the TiO_2 electrodes were observed. The anatase TiO_2 nanocrystals have six Raman active modes ($A_{1g} + 2B_{1g} + 3E_g$), which are located at 145 [$E_g(1)$], 197 [$E_g(2)$], 399 [$B1_g(1)$], 513 [$A1_g$], 519 [$B1_g(2)$], and 639 cm^{-1} [$E_g(3)$] [27]. Except for PREDCN2_Al_2O_3 coated on TiO_2, the Raman spectra were quite similar. Before adsorbing dyes, the Raman spectra of TiO_2 electrodes and Al_2O_3 coated TiO_2 electrode were almost identical in Fig. 4(a). After dye adsorbing on the TiO_2 electrodes and Al_2O_3 coated TiO_2 electrode, a low intensity of the vibration mode was generally observed. This proved that the chemical adsorption of dye on the surface of TiO_2 electrode and Al_2O_3 coated TiO_2 electrode [28]. Under resonant irradiation, the dye was very efficiently excited, and a large number of electrons were injected and then promoted to the TiO_2 conduction band. Hence, the surface charge increased strongly, and the TiO_2 electrode lost charge. In the case of the TiO_2 electrode with a

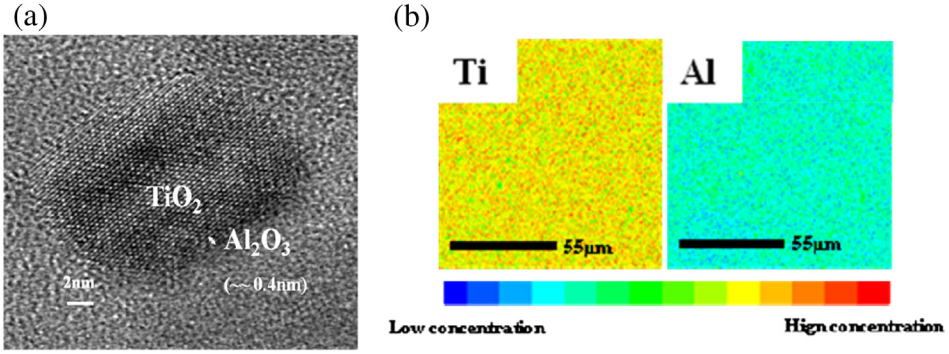

Fig. 2. (a) HR-TEM image of TiO_2 porous layer covered with Al_2O_3 (b) EPMA color mapping.

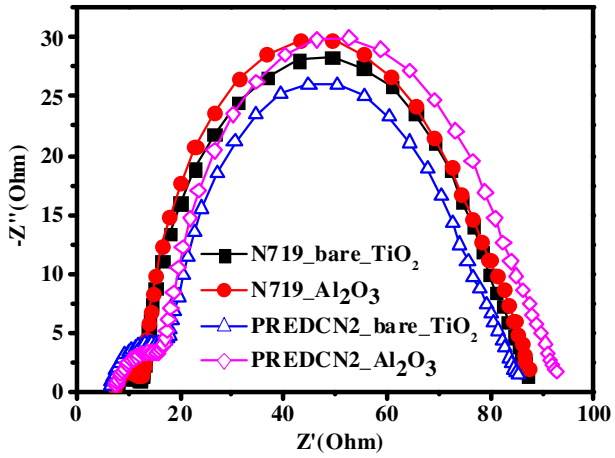

Fig. 3. Nyquist plots of DSSCs with and without an Al_2O_3 layer and different dyes.

PREDCN2_Al_2O_3 coating, the $E_g(3)$ mode of the TiO_2 phase significantly down-shifted from 637 to 605 cm^{-1}. This shift can be seen as the interaction between the dye and Al_2O_3 coated on the TiO_2 electrode through the carboxylic groups. To understand the cause of the shift, we compared the bare TiO_2 electrode with the Al_2O_3-coated TiO_2 electrode immersed in the PREDCN2 dye solution.

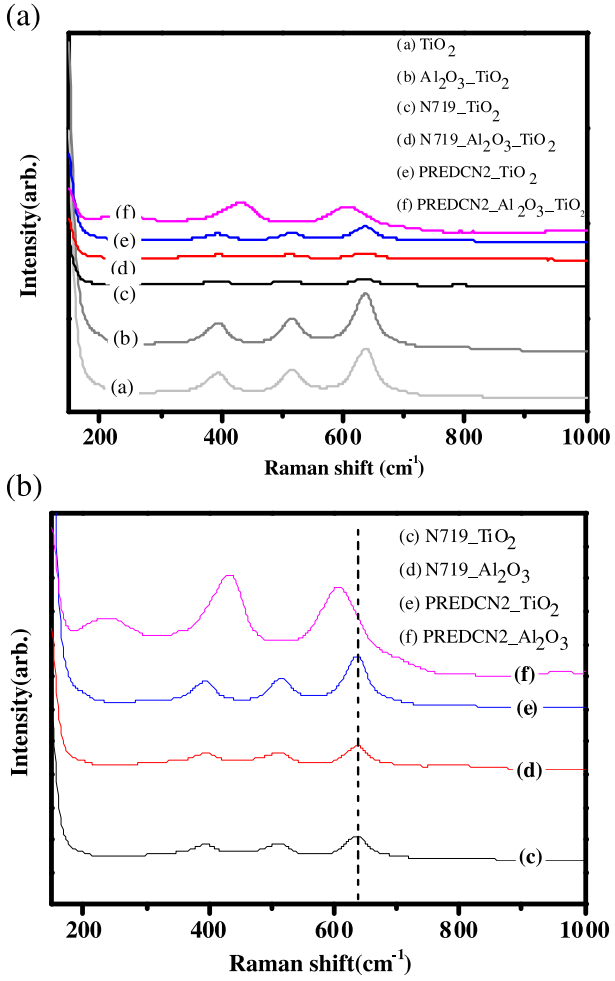

Fig. 4. (a) Raman spectra of TiO_2 electrode with and without Al_2O_3 layer and different dyes (b) Raman spectra of the structure layer.

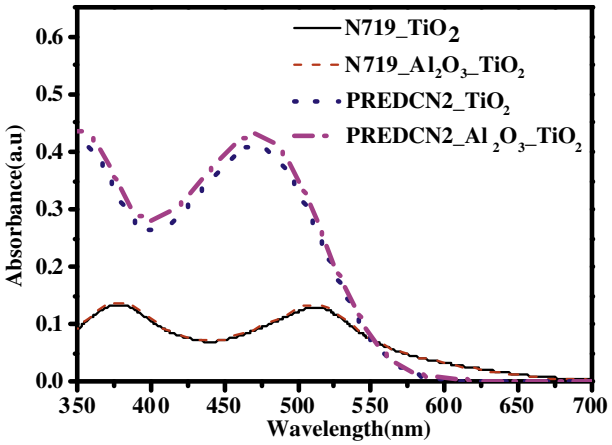

Fig. 5. Absorption spectra of dye desorbed from bare and Al_2O_3-coated TiO_2 samples using 0.1 M NaOH.

When PREDCN2 dye was adsorbed on the TiO_2 electrode, the intensities of the TiO_2 Raman peaks decreased, but no obvious Raman peak shifting was observed, as shown in Fig. 4(b). This result confirmed that the large Raman peak shifting of the Al_2O_3-coated TiO_2 electrode with PREDCN2 dye was mainly enhanced by the existing compact layer that decreased trapped.

To determine the amount of dyes adsorbed on bare TiO_2 and Al_2O_3-coated TiO_2 electrode at different dye, the dyes were desorbed from the TiO_2 photo-electrodes using 0.1 M NaOH, and the absorbance of the solution was measured with a UV–vis spectroscope. The results showed an improvement in dye adsorption with the Al_2O_3 layer, as shown in Fig. 5.

This was due to the carboxylic acid groups in the dye reacting more favorably with a surface with a more basic nature or a higher IEP, such as Al_2O_3 (~9.5), than with anatase TiO_2 (~5.5). This led to better light absorption [8,22], resulting in higher short-circuit photocurrent density (J_{sc}). In particular, the concentration of PREDCN2 (1.2×10^{-5} mmol cm^{-2}) was much higher than that of N719 (0.9×10^{-5} mmol cm^{-2}), which was in agreement with the adsorption properties of PREDCN2 shown in the Raman spectra measurements.

In order to explain the dye chemistry on current collection, we measured UV–vis absorption spectra of the dyes in DMF solution (Fig. 6).

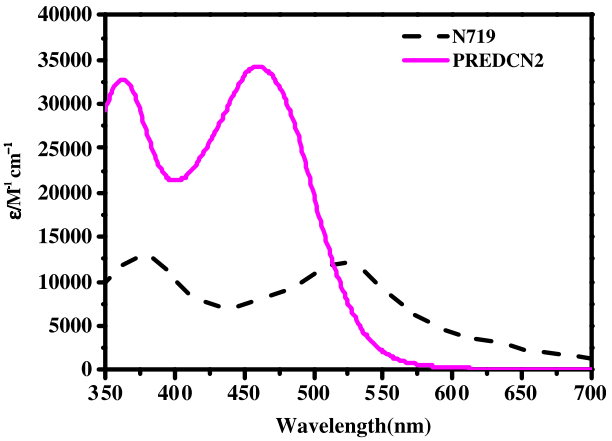

Fig. 6. Absorption spectra of N719 (black dashed line) and PREDCN2 (pink solid line) in DMF solution. (For interpretation of the references to colour in this figure legend, the reader is referred to the web version of this article.)

The visible absorption spectrum of PREDCN2 exhibited maxima at 459 nm ($\varepsilon = 34265\ M^{-1}\ cm^{-1}$) and which were attributed to the $\pi-\pi^*$ transitions of the conjugated molecules. Under similar conditions, N719 exhibited absorption bands at 524 nm ($\varepsilon = 12100\ M^{-1}\ cm^{-1}$). Organic dye had higher molar extinction coefficients than that of N719 [23a], and the highest occupied molecular orbital (HOMO) is usually used to estimate the efficiency of dye regeneration in DSSCs. To ensure regeneration of dye molecules, their HOMO level should be more positive than the redox potential of I^-/I_3^- in the electrolyte. The HOMO energy levels of the dye molecules were estimated by cyclic voltammetry; the results showed that PREDCN2 had more positive HOMO levels than the redox potential (+0.4 V) of I^-/I^{3-} in the electrolyte: +0.625 V and +0.827 V for PREDCN2 and N719, respectively. This indicates that organic dye can improve the light-harvesting efficiency or photogenerated electron–hole pairs.

3.2. Photovoltaic performance of DSSCs

The photovoltaic properties of DSSCs based on bare TiO_2 and Al_2O_3-coated TiO_2 were measured and compared to different dyes, as shown in Fig. 7 and Table 1.

The Al_2O_3-coated TiO_2 electrode performed better than the bare TiO_2 electrode with respective to all the cell parameters. Under the standard global AM 1.5 solar irradiation, J_{sc} increased from 10.3 to 12.9 mA cm^{-2}, V_{oc} increased from 640 to 710 mV, and the fill factor

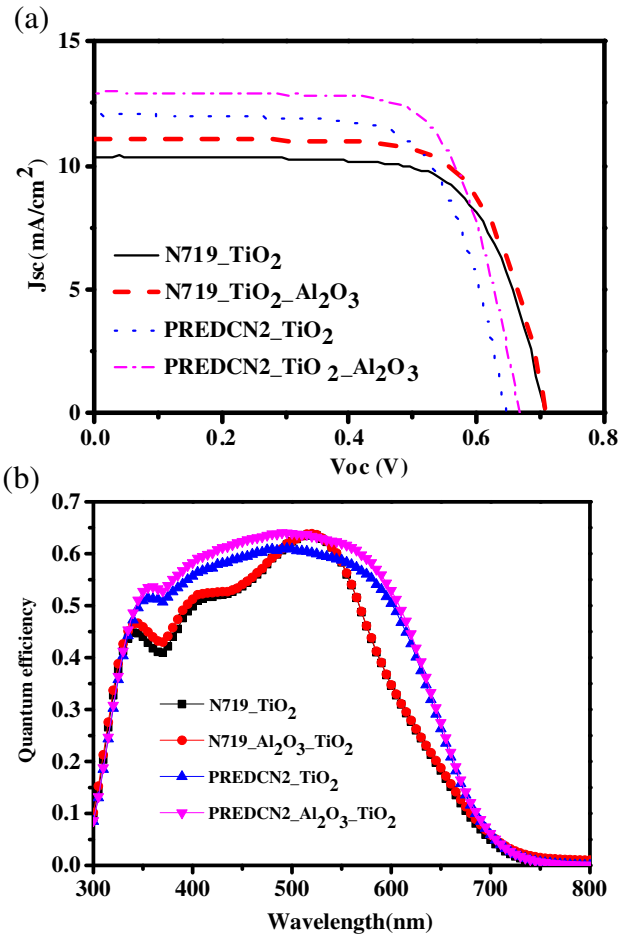

Fig. 7. (a) Current density–voltage characteristics for DSSCs containing different dyes under illumination of simulated solar light (AM 1.5, 100 mW cm^{-2}) (b) IPCE curves for DSSCs containing different dyes.

Table 1
Photovoltaic performance of DSSCs.[a]

Sample	J_{sc} (mA cm^{-2})	V_{oc} (V)	*FF* (%)	η (%)
N719[b]_TiO_2	10.377	0.708	70.43	5.17
N719[b]_Al_2O_3_TiO_2	11.093	0.711	70.44	5.55
PREDCN2[b]_TiO_2	12.049	0.647	69.9	5.45
PREDCN2[b]_Al_2O_3_TiO_2	12.956	0.668	71.03	6.15

[a] Photovoltaic performance under AM 1.5 irradiation of DSSCs containing N719 and PREDCN2 dyes, based on 3-propyl-1-methyl-imidazolium iodide (PMII, 1 M), lithium iodide (LiI, 0.2 M), iodide (I_2, 0.05 M), and *tert*-butylpyridine (TBP, 0.5 M) in acetonitrile/valeronitrile (85:15).
[b] Dye bath: ethanol solution (3×10^{-4} M).

(*FF*) increased from 0.69 to 0.71, corresponding to an overall conversion efficiency (η) increase from 5.1 to 6.1%. The increases in V_{oc} and fill factor were consistent with previous reports on DSSCs using liquid electrolytes owing to the blocking of interfacial recombination [14].

The increase in J_{sc} is more interesting considering the possible disadvantages of an insulator interlayer for electron injection. The results shown here demonstrated that the surface-solution process was a suitable way to fabricate an insulator interlayer for DSSCs. The Al_2O_3 layer prepared was very thin that electrons could be injected efficiently from the photo-excited dye molecules to the TiO_2 electrode by tunneling. In addition, the higher photocurrent density of PREDCN2 than N719 could be explained by the high molar extinction coefficient and adsorption property of PREDCN2. This is due to EDOT unit in PREDCN2 has not only a small torsion angle with respect to the adjoining phenyl fragment, ensuring efficient electronic communication between donor and acceptor but also planarity of the π-conjugation structure and the adsorption of the sensitizers on the electrode, which could contribute to the electron injection from the excited state [23b] (Fig. 7).

The incident photon-to-current efficiency (IPCEs) properties of DSSCs based on bare TiO_2 and Al_2O_3-coated TiO_2 were measured and compared to different dyes. A higher photon-to-current efficiency was achieved in the DSSC based on the PREDCN2 compared to N719 dye. And also, IPCEs of bare TiO_2 was lower than that of Al_2O_3-coated TiO_2 electrode. This was primarily due to the higher J_{sc}, as shown in Table 1. The IPCE for the PREDCN2 based on Al_2O_3-coated TiO_2 cell reached about 65% in the 400–600 nm wavelength range. The enhanced cell efficiency of DSSCs containing PREDCN2 may be due to high molar extinction coefficients and adsorption property, which is $\pi-\pi$ interactions could be attributed to higher electron injection and light harvesting efficiency.

To clarify the differences between the behavior in DSSCs based on N719 and PREDCN2, we used IMPS and IMVS to investigate the electron transport kinetics related to the electron diffusion coefficient (D_e) and lifetime (τ_e), as shown in Fig. 8. The detailed parameters are listed in Table 2.

The values of D_e and τ_e were determined by the photocurrent and photovoltage transients induced by a stepwise change in the laser light intensity, controlled with a function generator [24]. The D_e value was obtained by a time constant (τ_c) determined by fitting the decay of the photocurrent transient with exp ($-t/\tau_c$) and the TiO_2 film thickness (ω) with $D_e = \omega^2/(2.77\tau_c)$ [23a]. The τ value was also determined by fitting the decay of photovoltage transient with exp ($-t/\tau$).

Fig. 8(a) shows that the values of D_e is greatly different in the DSSCs with dyes at the same short-circuit current densities. Nakade et al. previously observed that the adsorption of N719 onto a TiO_2 electrode increased the D_e value compared to a bare TiO_2 electrode, and they attributed this increase to a decrease in the number of trapping sites on the TiO_2 surface owing to dye adsorption [25]. In the case of the PREDCN2 on the Al_2O_3-coated TiO_2 electrode,

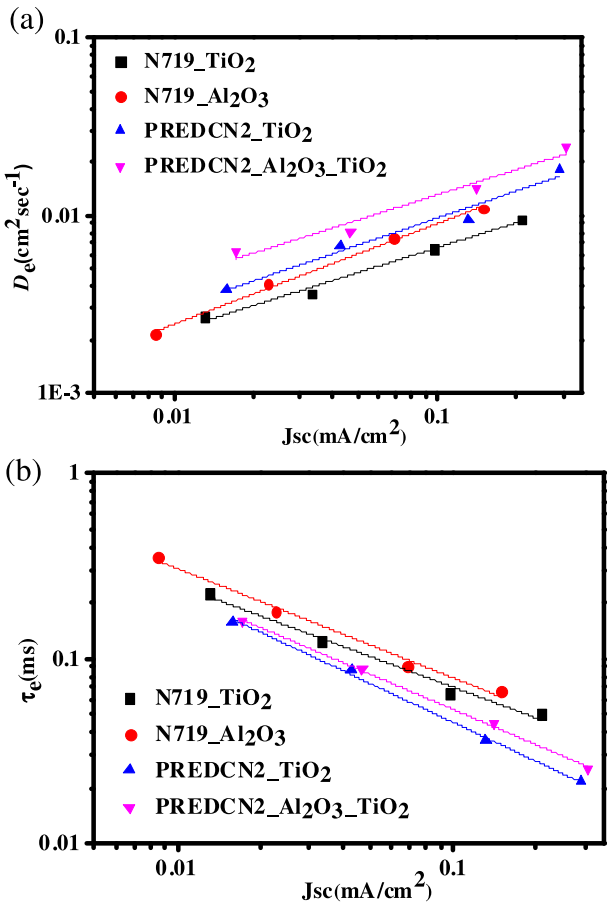

Fig. 8. (a) Diffusion coefficients (D_e) and (b) electron lifetimes (τ_e) obtained for DSSCs based on N719 and PREDCN2 dyes as a function of short-circuit photocurrent density (J_{sc}).

the electron diffusion coefficient reached the highest value (24.4×10^{-3}). This not only decreased trapping by the Al_2O_3 layer, it also increased the tunneling effect. Moreover, the high molar extinction coefficient and efficient electron extraction paths owing to the adsorption property of PREDCN2 were beneficial to faster electron transport, indicating that PREDCN2 on the Al_2O_3-coated TiO_2 electrode could improve charge injection and collection efficiency and thus increase photovoltaic-conversion efficiency. Fig. 8(b) shows that the values of electron lifetime (τ_e) of N719 were drastically enhanced, compared with those of PREDCN2, with the help of the hydrophobic aliphatic chains [26] and larger molecular size retarding the electron recombination, which originated from direct contact between the electrons on the TiO_2 surface and I^{3-} ions in the electrolyte. The values of the electron lifetime were also consistent with those of V_{oc} shown in Table 1.

From these results, it can be seen that the electron diffusion length, L_n ($=(D_e\tau_e)^{0.5}$), would be affected more markedly by changing the value of τ_e, rather than changing the value of D_e. The τ_e values of both N719 and PREDCN2, however, were enhanced by the insertion of the Al_2O_3 layer compared to the cell without the Al_2O_3 layer.

As a result, the charge-collection efficiency (η_{cc}) for PREDCN2 dye on the Al_2O_3-coated TiO_2 electrode, as described by the relationship $\eta_{cc} = 1 - (\tau_c/\tau_e)$, is much greater. Table 2 shows that η_{cc} for PREDCN2 is 5% larger than that for the N719. Therefore, PREDCN2 can not only enhance the light-harvesting efficiency, it also increases the charge-collection efficiency and can influence the photocurrent density (J_{sc}).

Table 2
Detailed IMPS/IMVS parameters of DSSCs with N719 and PREDCN2 dyes.

Sample	D_e (cm^2 s^{-1})[a]	L_n (μm)[b]	η_{cc} (%)[c]
N719_TiO$_2$	9.58×10^{-3}	6.92	66.3
N719_Al$_2$O$_3$_TiO$_2$	10.97×10^{-3}	7.17	70.2
PREDCN2_TiO$_2$	18.1×10^{-3}	6.2	61.2
PREDCN2_Al$_2$O$_3$_TiO$_2$	24.4×10^{-3}	7.8	75.2

[a] D_e, diffusion coefficient.
[b] L_n, diffusion length.
[c] η_{cc}, charge-collection efficiency.

4. Conclusions

In the study reported here, we investigated the improvement in performance of dye-sensitized solar cells (DSSCs) by coating ultrathin metal oxides (Al_2O_3) on mesoporous TiO_2 electrodes using the solution process. The Al_2O_3 layers were highly effective at reducing recombination at the TiO_2–dye–electrolyte interface, increasing J_{sc} caused by decreased trapping. This indicated an overall increase in device efficiency attributed to more efficient electron injection. Furthermore, the importance of dye choice was also demonstrated, in which the current density was much more enhanced by a metal-free organic dye than the Ru dye. The π–π^* transitions of the conjugated molecule in the metal-free organic dye provided a higher molar extinction coefficient and more efficient electron injection from the dye to TiO_2 conduction band, resulting in an increase in the diffusion coefficient of the solar cell and an increase in J_{sc}. Even though lower voltages in DSSCs based on organic dyes compared to those based on Ru dye resulted from shorter τ_e values, a high diffusion coefficient of the organic dye provided fast electron injection, resulting in an increase in charge-collection efficiency.

Acknowledgments

This research was supported by a grant from the Fundamental R&D program for Core Technology of Materials (10037239) funded by the Ministry of Knowledge Economy, Republic of Korea. It was also supported by the DGIST R&D Program of the Ministry of Education, Science and Technology of Korea (13-EN-04).

References

[1] B. O'Regan, M. Grätzel, Nature 353 (1991) 737.
[2] M. Grätzel, Nature 338 (2001) 414.
[3] M.K. Nazeeruddin, A. Kay, I. Rodicio, R. Humphry-Baker, E. Mueller, P. Liska, N. Valchopoulos, M. Grätzel, J. Am. Chem. Soc. 115 (1993) 6382.
[4] M.K. Nazeeruddin, S.M. Zakeeruddin, R. Humphry-Baker, M. Jirousek, P. Liska, N. Vlachopoulos, V. Shklover, C.-H. Fischer, M. Grätzel, Inorg. Chem. 38 (1999) 6298.
[5] M. Grätzel, Inorg. Chem. 44 (2005) 6841.
[6] E. Palomares, J.N. Clifford, S.A. Haque, T. Lutz, J.R. Durrant, Chem. Commun. 125 (2002) 1464.
[7] J.R. Durrant, S.A. Haque, E. Palomares, Coord. Chem. Rev. 248 (2004) 1247.
[8] E. Palomares, J.N. Clifford, S.A. Haque, T. Lutz, J.R. Durrant, J. Am. Chem. Soc. 125 (2003) 475.
[9] Z.S. Wang, M. Yanagida, K. Sayama, H. Sugihara, Chem. Mater. 18 (2006) 2912.
[10] S. Lee, J.Y. Kim, K.S. Hong, H.S. Jung, J.K. Lee, H. Shin, Sol. Energy Mater. Sol. Cells 90 (2006) 2405.
[11] L. Zhang, Y. Shi, S. Peng, J. Liang, Z. Tao, J. Chen, J. Photochem. Photobiol. A. 197 (2008) 260.
[12] V. Ganapathy, B. Karunagaran, S.-W. Rhee, J. Power Sources 195 (2010) 5138.
[13] T.-C. Tien, F.-M. Pan, L.-P. Wang, C.-H. Lee, Y.-L. Tung, S.-Y. Tsai, C. Lin, F.-Y. Tsai, S.-J. Chen, Nanotechnology 20 (2009) 305201.
[14] (a) A. Kay, M. Grätzel, Chem. Mater. 14 (2002) 2930;
(b) J. Yu, J. Fan, B. Cheng, J. Power Sources 196 (2011) 7891;
(c) J. Fan, S. Liu, J. Yu, J. Mater. Chem. 22 (2012) 17027;
(d) J. Yu, Q. Li, Z. Shu, Electrochim. Acta 56 (2011) 6293.
[15] S.S. Zhu, T.M. Swager, J. Am. Chem. Soc. 119 (1997) 12568.
[16] A.W. Franz, F. Rominger, T.J.J. Mller, J. Org. Chem. 73 (2008) 1795.

[17] Y.S. Yang, H.D. Kim, J.H. Ryu, K.K. Kim, S.S. Park, K.S. Ahn, J.H. Kim, Synth. Metal. 161 (2011) 850.
[18] J. Bisquert, F. Fabregat-Santiago, I. Mora-Seró, G. Garcia-Belmonte, S. Giménez, J. Phys. Chem. C 113 (2009) 17278.
[19] J. Van de Lagemaat, N.G. Park, A.J. Frank, J. Phys. Chem. B 104 (2000) 2044.
[20] Q. Wang, J. Moser, M. Grätzel, J. Phys. Chem. B 109 (2005) 14945.
[21] P. Qu, G.J. Meyer, Langmuir 17 (2001) 6720.
[22] (a) S.M. Zakeeruddin, R. Humphry-Baker, P. Pechy, P. Quagliotto, C. Barolo, G. Viscard, M. Grätzel, Langmuir 18 (2002) 952;
(b) G. Zhang, H. Bala, Y. Cheng, D. Shi, X. Lv, Q. Yu, P. Wang, Chem. Commun. 0 (2009) 2198.
[23] (a) S. Nakade, T. Kanzaki, Y. Wada, S. Yanagida, Langmuir 21 (2005) 10803;
(b) K.S. Ahn, M.S. Kang, J.-K. Lee, B.-C. Shin, J.W. Lee, Appl. Phys. Lett. 89 (2006) 013103.
[24] S. Nakade, Y. Saito, W. Kubo, T. Kanzaki, T. Kitamura, Y. Wada, S. Yanagida, Electrochem. Commun. 5 (2003) 805.
[25] K. Hara, K. Miyamoto, Y. Abe, M. Yanagida, J. Phys. Chem. B 109 (2005) 23776.
[26] M. Micami, S. Nakamura, O. Kitao, H. Arakawa, Phys. Rev. B Condens. Matter Mater. Phys. 66 (15) (2002) 1552131.
[27] C. Perez Leon, L. Kador, B. Peng, M. Thelakkat, J. Phys. Chem. B 110 (17) (2006) 8723.